Internal State Estimation Based on Facial Images with Individual Feature Separation and Mixup Augmentation

Ayaka Asaeda and Noriko Takemura[a]

Kyushu Institute of Technology, Fukuoka, Japan

Keywords: Mixup Augmentation, Drowsiness Estimation, Feature Separation.

Abstract: In recent years, the opportunity for e-learning and remote work has increased due to the impact of the COVID-19 pandemic. However, issues such as drowsiness and decreased concentration among learners have become apparent, increasing the need to estimate the internal state of learners. Since facial expressions reflect internal states well, they are often utilized in research on state estimation. However, individual differences in facial structure and expression methods can influence the accuracy of these estimations. This study aims to estimate ambiguous internal states such as drowsiness and concentration by considering individual differences based on the Deviation Learning Network (DLN). Such internal states exhibit very subtle and ambiguous changes in facial expressions, making them more difficult to estimate compared to basic emotions. Therefore, this study proposes a model that uses mixup, which is one form of data augmentation, to account for subtle differences in expressions between classes. In the evaluation experiments, facial images of learners during e-learning will be used to estimate their arousal levels in three categories: Asleep, Drowsy, and Awake.

1 INTRODUCTION

The COVID-19 pandemic has led to an increase in e-learning, allowing educational activities to be conducted from home. In the workplace, an increasing number of companies are introducing remote work, allowing employees to perform their tasks from home without the need to commute to the office. However, remote work can cause fatigue and drowsiness from long hours of sitting and watching videos, decreased concentration due to the lack of people around, and reduced tension.To prevent such situations, systems that estimate the user's state and provide alerts have gained attention in recent years. For the development of such systems, accurately understanding the user's internal state is crucial. Various sensing data, such as facial expressions, heart rate, and brain activity, are used to estimate internal states. Among them, facial expressions have been used in many state estimation studies because they contain much information about the human mental state, and it is easy to collect the data(Kim et al., 2019)(Zhang et al., 2019). However, there are issues with using facial expressions for state estimation. Typical facial features such as eyebrows, eyes, nose, and mouth differ in size, spacing, angles, and shapes from person to person. Such individual differences in facial structure are crucial for individual identification but may negatively impact facial expression recognition accuracy. In addition to structural differences, it is also known that cultural differences can cause variations in how facial expressions are displayed and their intensity, leading to individual differences in expression(Friesen, 1973). One possible way to reduce the effects of such individual differences is to collect facial image data from many people, but this is not readily achievable due to privacy and ethical issues. In addition, to construct a state estimation model by machine learning, labels of internal states are required for each data set. However, the time and financial cost of annotation is high, and the larger the dataset, the greater the cost in proportion. Therefore, this research aims to estimate human states with a small dataset, considering individual differences. Although there have been various approaches to reduce the influence of individual differences in facial expression recognition, most of the previous studies have focused on basic emotions, which are relatively easy to estimate(Xie et al., 2021; Liu et al., 2019; Meng et al., 2017). However, it is essential to estimate ambiguous internal states such as concentration, drowsiness, and fatigue, in addition to simple and clear emotion estimation when considering the

[a] https://orcid.org/0000-0003-1977-4690

Asaeda, A. and Takemura, N.
Internal State Estimation Based on Facial Images with Individual Feature Separation and Mixup Augmentation.
DOI: 10.5220/0013161900003912

In *Proceedings of the 20th International Joint Conference on Computer Vision, Imaging and Computer Graphics Theory and Applications (VISIGRAPP 2025) - Volume 2: VISAPP*, pages 911-918
ISBN: 978-989-758-728-3; ISSN: 2184-4321

application to actual systems. Since ambiguous internal states are not easily expressed in facial expressions and their minute changes, they are more affected by individual differences than basic emotions. In this study, we aim to estimate ambiguous internal states while accounting for individual differences in facial expression recognition using the Deviation Learning Network (DLN) (Zhang et al., 2021). The DLN's deviation module extracts individual-independent facial features by subtracting individual-specific features. Since ambiguous expressions vary by individual and situation, their features cannot be uniquely defined, requiring diverse data for accurate identification. However, annotating such subtle changes, especially for intermediate states, is challenging. To address this, we propose a model learning method that generates intermediary data between classes using the *mixup* (Zhang et al., 2018) data augmentation technique.

In the evaluation experiment, we estimated drowsiness levels (Awake, Drowsy, and Asleep), using face image data from 27 e-learning participants.

2 STATE ESTIMATION SEPARATING INDIVIDUAL FEATURES

2.1 Facial Region Extraction Method

The Multi-task Cascaded Convolutional Neural Networks (MTCNN)(Zhang et al., 2016) was used to create face image data (160×160 pixels) by extracting the face regions of the learner in the image data. MTCNN is a facial detection method composed of three stages of CNNs: the Proposal Network (P-Net), which detects facial regions; the Refine Network (R-Net), which removes non-facial areas from the candidates based on the outputs of the P-Net; and the Output Network (O-Net), which detects parts such as the eyes, nose, and mouth, and ultimately outputs the facial regions. Faces smaller than a certain minimum detection size were excluded to ensure that even if other people appear in the background behind the learner, only the learner's face is targeted for detection. MTCNN cannot detect a face if the person to be estimated is looking down from a certain angle. In some cases, more than one person appeared in the image, so the faces of non-target persons were removed based on the size of the face area and similarity information. An example of MTCNN applied to image data is shown in Figure 1.

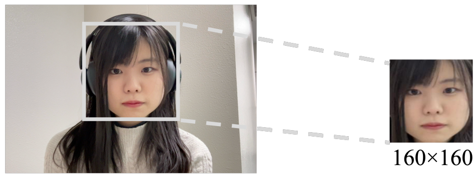

Figure 1: Examples of face region extraction using MTCNN.

2.2 State Estimation Method

The proposed method introduces a state estimation model that considers individual differences. It consists of a deviation module for separating individual features and a state estimation module that estimates the internal state based on the output of the features by the deviation module. The overview of the state estimation method is shown in Figure 2. Further details on both the deviation and state estimation modules will be provided.

Deviation Module. In the deviation module, an individual identification model (Identity Model) and a face recognition model (Face Model) are used as parallel networks to extract internal state features independent of individuals. First, the Identity Model uses a pre-trained model called FaceNet(Schroff et al., 2015) to extract individual features. FaceNet is designed to learn optimal embeddings of facial features extracted from images into an Euclidean space. By calculating the distances between faces in this generated space, the method facilitates the determination of facial similarities. For pre-training the Identity Model, the VggFace2 dataset(Cao et al., 2018), comprising face images of 9,131 individuals (approximately 3.31 million images) encompassing diverse ages and ethnicities, is utilized. The CNN constituting Identity Model employs the Inception Resnet (v1)(Szegedy et al., 2017) as in FaceNet. Subsequently, we prepared a Face Model with the same structure and weights as the Identity Model to establish a parallel network. During the training of this network, the weights of the Identity Model are fixed, and the Face Model is trained. The 512-dimensional state feature vector V_{state} that is independent of the individual is obtained by subtracting the individual feature vector V_{id} (512-dimensional), outputted from the Identity Model from the facial image feature vector V_{face} (512-dimensional), outputted from the Face Model. It is formulated as in equation (1).

$$V_{\text{state}} = V_{\text{face}} - V_{\text{id}} \tag{1}$$

State Estimation Module. The state estimation module uses the 512-dimensional state feature vector V_{state} obtained from the deviation module to output features

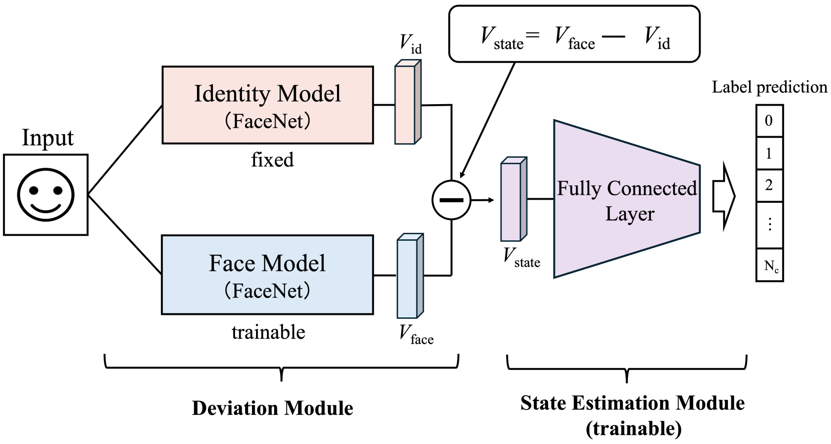

Figure 2: Overview of the proposed method for state estimation separating individual features.

of N_c dimensions (where N_c represents the number of state classes) as its final layer for estimating internal states. This module comprises two fully connected layers that reduce dimensions from 512 to 128 and then to N_c dimensions. Activation functions Rectified Linear Unit and Dropout (with a selection rate of 0.4) are applied in each layer. The final layer employs a Softmax function, and the loss function used is the cross-entropy loss.

3 DATA AUGMENTATION WITH *MIXUP*

3.1 Mixed Data Generation Method

Mixup is a data augmentation technique that mixes two images. In this study, we expect to improve the model's generalization performance by generating data intermediate between the two classes that are difficult to distinguish and increasing the data around the class boundaries. The mixing process for creating a mixed data $\tilde{x}_{ij}$ and mixed label $\tilde{y}_{ij}$ from data i (image x_i, label y_i) and data j (image x_j, label y_j) using the mixing ratio λ is formulated as in equations as follows.

$$\tilde{x}_{ij} = \lambda x_i + (1-\lambda) x_j \quad (2)$$
$$\tilde{y}_{ij} = \lambda y_i + (1-\lambda) y_j \quad (3)$$

Figure 3 shows an example of a mixed image applying *mixup* using the drowsiness level labeled images used in the evaluation experiment. Figure 4 displays a t-SNE visualization of the feature vectors for both pre-mixed and mixed data (using $\beta(2,2)$), illustrating the distribution of the data in a reduced-dimensional space.

Figure 3: Examples of applying *mixup* to facial images.

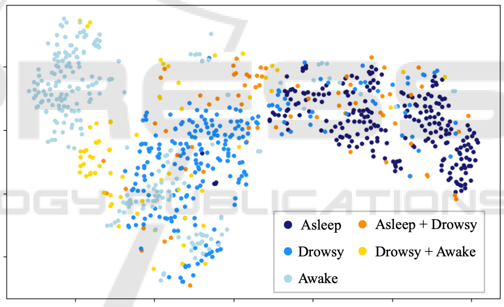

Figure 4: Visualization of feature vectors including *mixup* data with t-SNE.

In this study, we also evaluate the performance of mixing feature vectors output by the deviation module in addition to mixing images. As in the case of images, *mixup* is applied using equation (2) and equation (3) (where x is the feature vector).

3.2 State Estimation with Mixed Images

When training the state estimation model, the training data is augmented by generating a mixture of two images with different labels. The network structure described in Section 2 (Figure 2) uses the Vggface2 dataset for pre-training the Identity Model, which may not extract individual features correctly when mixed images are input. Therefore, the Identity Model is added as a parallel network in the deviation module, and two Identity Models and one Face

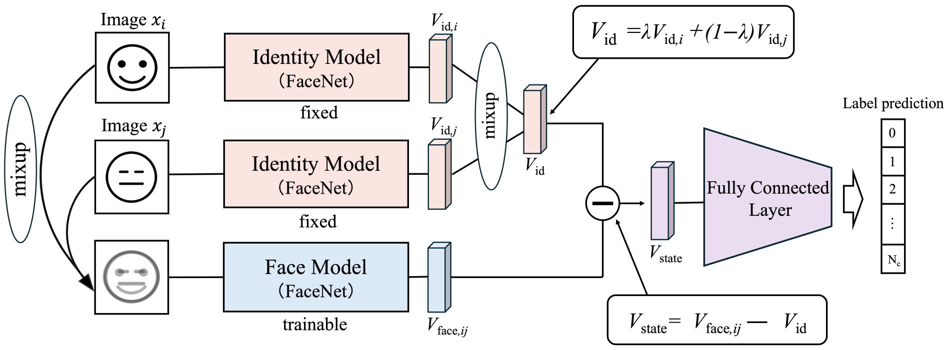

(a) Applying *mixup* to facial images

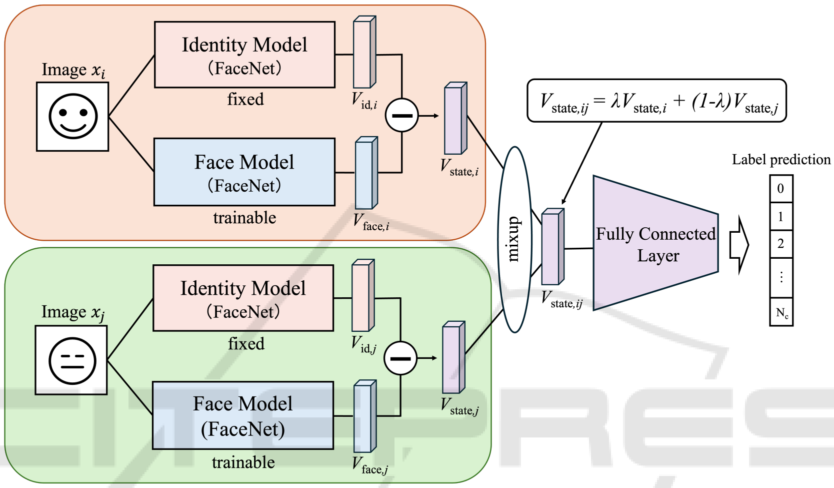

(b) Applying *mixup* to feature vectors

Figure 5: Overview of the state estimation model using *mixup*.

Model are used for training. The overview of the network is shown in Figure 5(a). The two pre-mixed facial image data x_i and x_j are inputted for the Identity Model. Based on the mixing ratio λ, individual feature vectors $V_{\text{id},i}$ and $V_{\text{id},j}$ that include individual features from each facial image data are calculated(equation (2)). The Face Model inputs the mixed image, blended based on the mixing ratio λ, to obtain the facial image feature vector $V_{\text{face},ij}$. Then, the individual feature vector V_{id} is subtracted from the face image features $V_{\text{face},ij}$, and the obtained state features vector V_{state} are used to estimate the state in the state estimation module.

3.3 State Estimation with Mixed State Feature Vector

The results were verified not only in the case of blending two images, but also in the case of blending feature vectors extracted from each image. For each of the two face image data x_i and x_j, the state feature vectors $V_{\text{state},i}$ and $V_{\text{state},j}$ are obtained by the deviation module shown in Figure 2. These are blended using *mixup* to obtain $V_{\text{state},ij}$(equation (2)). After that, $V_{\text{state},ij}$ is input to the state estimation module to estimate the state, as described in Section 2. The overview of the network is shown in Figure 5(b).

4 EVALUATION EXPERIMENTS

4.1 Datasets

We collected video data of 53 undergraduate students learning about information science by e-learning. The subjects were 17 males and 36 females of East Asian descent, with varying hairstyles and clothing. They viewed the lecture videos(slides + audio) on a laptop and were recorded from the front, capturing their upper body using the laptop's built-in camera, as shown in Figure 1. The data collection experiment was conducted over four days, with each subject view-

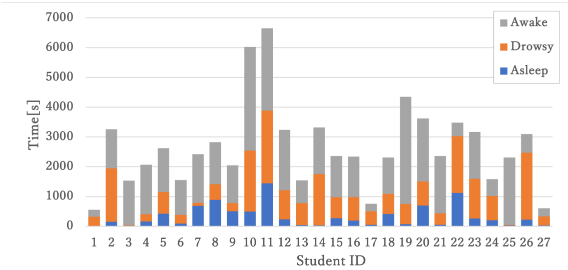

Figure 6: Distribution of each drowsiness state(Before undersampling).

Table 1: Coding scheme of drowsiness state.

Label	Scheme
Asleep	- Eyes are closed over 1 second
Drowsy	- Eyes are not always open - Pupils do not move - Eyes are closed for less than 1 second - Body movements and head poses are uncontrolled
Awake	- Eyes are wide open - Pupils move to the right and left - Body movements and head poses are under control

ing 1 to 3 lecture videos (about 10 minutes each) daily. However, since each subject attended only the days they could, the total number of data varied per subject.The captured image size was 640×480 pixels with a frame rate of 10fps. A single annotator manually annotates the drowsiness level of the subject while watching the video of the subject learning and the lecture video. In the annotation process, the annotator labeled the drowsiness level of the learners (Asleep/Drowsy/Awake) every second based on their state in continuous videos. Drowsiness levels were annotated based on the criteria shown in Table 1. In this study, we performed an evaluation experiment using a three-class classification based on the images for the 27 subjects who had data for all labels (Asleep/Drowsy/Awake). A breakdown of the data for each label by subject is shown in Figure 6.

4.2 Comparative Methods

In this experiment, we evaluate the model's performance with and without individual feature separation, with and without *mixup*, and by its application method.

4.2.1 Comparison with and Without Individual Feature Separation

This experiment compares the proposed method, which estimates drowsiness using state features separated from individual features via the deviation module (Figure 2), with a method that does not separate features. The comparative method directly extracts features from input images using only the Face Model and estimates drowsiness, with its initial weights identical to those in the proposed method. An overview of the comparative method is shown in Figure 7.

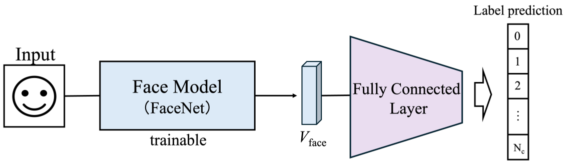

Figure 7: Overview of the comparative method without the deviation module.

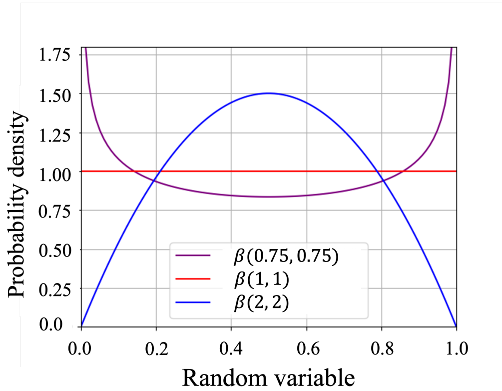

Figure 8: Graph of the beta distribution.

4.2.2 Comparison Based on *Mixup* Application Method

Accuracy comparisons are conducted for the state estimation model that separates individual features based on whether *mixup* is applied and the method of its application (across four specified patterns). In this experiment, for the combination of classes to apply *mixup*, we mixed the images and state features of the Asleep-Drowsy and Drowsy-Awake classes, which have relatively close features between the classes. In this experiment, mixed data is used only for the training set, while the validation and test data consist solely of the original data (Asleep/Drowsy/Awake) without any mixing.

Comparison Based on the Stage of *Mixup*. Application We compare two patterns for the *mixup* application stages. The first is to mix the images directly before input (Figure 5(a)). The other method is to mix feature vectors (Figure 5(b)).

Comparison Based on the Subject of *Mixup*. Application The model performance is compared for

Table 2: Number of samples in each group for cross-validation.

	Asleep	Drowsy	Awake
group1	1,810	1,811	1,810
group2	5,934	5,934	5,934
group3	6,002	6,002	6,002
group4	15,165	15,165	15,165
group5	2,109	2,110	2,109
group6	4,822	4,822	4,822
group7	5,336	5,336	5,336
group8	8,859	8,859	8,860
group9	2,800	2,880	2,880

Table 3: Comparison of macro-F1 scores with and without the deviation module.

Method	macro-F1
w/ DM* (Ours)	**0.535**
w/o DM	0.523

*DM: Deviation Module

two patterns of *mixups*: mixing the same and different persons.

Comparison Based on the Number of *Mixups*. The number of mixed data with *mixups* used for the training data is compared for accuracy in 5 patterns: 0%, 10%, 20%, 30%, and 40% of the original data.

Comparison Based on the *Mixup* Ratio. Randomly generates values of λ based on the beta distribution. Three patterns of beta distributions were set up with different shapes: $Beta(0.75, 0.75)$, $Beta(1, 1)$ and $Beta(2, 2)$. A graph of the beta distribution is shown in Figure 8.

4.3 Evaluation Methods

The 27 participants were divided into nine groups of three, and leave-one-group-out cross-validation was performed. One group was used as test data, another as validation data, and the remaining seven as training data. This process was repeated nine times so each group served as test data once, and performance was evaluated by averaging the nine results. Table 2 shows the label distribution in each group. To address label imbalance, face images for training were undersampled per subject. The macro-F1 score, the average of F1 scores across classes, was used as the evaluation metric. Mini-batch learning was applied with a batch size of 128. Models were trained for 1500 batches and evaluated on test data. The initial learning rate was 0.001 and reduced by a factor of 0.1 at the end of each epoch (approximately 1000 batches). Weight decay of 0.001 was used to prevent overfitting, and Stochastic Gradient Descent (SGD) was employed as the optimizer. A fixed seed ensured reproducibility, and the same pairs were mixed when generating mixed data.

Table 4: Comparison of macro-F1 scores with and without *mixup* ($\beta(0.75, 0.75)$).

Method	Pair	macro-F1
w/o *mixup*	-	0.535
mixup Images	Other	0.537
	Same	0.549
mixup V_{state}	Other	0.550
	Same	**0.569**

4.4 Evaluation Results

4.4.1 Comparison with and Without Individual Feature Separation

Table 3 shows the macro-F1 score results for cases where state estimation was conducted with individual features separated using the deviation module, compared to direct state estimation from facial images without using the deviation module. A comparison of accuracy with and without individual feature separation showed that the proposed method with individual feature separation improved accuracy. This indicates that separating individual features from facial image features and extracting state features independent of the individual is effective for estimating ambiguous internal states.

4.4.2 Comparison with and Without *Mixup* and Its Application Methods

Table 4 shows the macro-F1 score results with and without *mixup*, as well as different application methods, when individual features are separated using the deviation module. The amount of mixed data added was set to 10%, with the *mixup* ratio determined by the beta function $\beta(0.75, 0.75)$. The results indicate that applying *mixup* increases accuracy across all patterns compared to not applying it, demonstrating its effectiveness in the proposed model. Confusion matrices for cases with and without *mixup* (mixing the same individuals, V_{state}) are shown in Table 5, which presents the cumulative results of nine cross-validation rounds. Table 5 also highlights that *mixup* improves identification accuracy for Asleep-Drowsy and Drowsy-Awake transitions.

Comparison Based on the Stage of *Mixup* Application. Comparing the stages of the *mixup* application, higher accuracy was obtained when feature vectors were mixed than when images were mixed. This could be because directly mixing images might

Table 5: The confusion matrices with and without *mixup* (mixing the same persons, V_{state}).

		Preds			Recall
		Asleep	Drowsy	Awake	
True	Asleep	42,685	5,515	4,637	0.808
	Drowsy	9,178	15,950	27,710	0.302
	Awake	5,229	16,608	31,000	0.587
Precision		0.748	0.419	0.489	F1:0.535

(a) Without *mixup*

		Preds			Recall
		Asleep	Drowsy	Awake	
True	Asleep	44,977	4,629	3,231	0.851
	Drowsy	9,753	16,651	26,434	0.315
	Awake	5,042	15,476	32,319	0.612
Precision		0.752	0.453	0.521	F1:0.569

(b) With *mixup*

Table 6: Comparison of macro-F1 scores based on the beta distribution parameter.

Method	Pair	$\beta(0.75, 0.75)$	$\beta(1,1)$	$\beta(2,2)$
mixup Images	Other	0.537	0.537	0.537
	Same	0.549	0.549	0.549
mixup V_{state}	Other	0.550	0.550	0.550
	Same	**0.569**	**0.569**	0.568

Table 7: Comparison of macro-F1 scores when changing the number of *mixups*.

Method	Pair	0%	**10%**	20%	30%	40%
w/o *mixup*		0.535	-	-	-	-
mixup Images	Other	-	**0.537**	0.536	0.536	0.532
	Same	-	**0.549**	0.539	0.536	0.529
mixup V_{state}	Other	-	**0.550**	0.548	0.549	0.547
	Same	-	**0.569**	0.565	0.556	0.558

include unnecessary information for the model's estimations, making it harder to identify the essential features. On the other hand, mixing state feature vectors, which only handle the feature of drowsiness already separated from individual features in the deviation module, likely include less irrelevant information. This makes it easier to extract the crucial information related to state estimation.

Comparison Based on the Subject of *Mixup* Application. Comparing the results for the *mixup* pairs, better accuracy was achieved when mixing the same person than when mixing different persons, both mixing images directly and mixing feature vectors. This is likely because when mixing different persons, not only are the features of different classes mixed due to the *mixup*, but also the features of different individuals are mixed together, which prevents effective learning of the model for state estimation.

4.4.3 Ablation Study

Comparison Based on the *Mixup* Ratio. Table 6 shows the results of the beta distribution for three patterns of mixing ratio λ: $\beta(0.75, 0.75)$, $\beta(1,1)$ and $\beta(2,2)$. The accuracy did not change significantly under each condition, likely because the added mixture data is relatively small (about 10%).

Comparison Based on the Number of *Mixups* Table 7 shows the results of incrementally adding *mixup* data as training data to find the optimal amount. With the beta distribution set to $\beta(0.75, 0.75)$, adding 10% *mixup* data achieves the highest accuracy, after which accuracy declines with further increases. This suggests that while *mixup* is effective, finding the optimal proportion is crucial, as excessive amounts reduce accuracy.

Table 8: Comparison of the individual identification accuracy with and without the deviation module.

Method	Accuracy
w/ DM (Ours)	**0.633**
w/o DM	0.830

4.5 Verification of Individual Features Separation

To verify whether the deviation module effectively separates individual features, we compare the individual identification accuracy of the proposed method (Figure 2) and the comparative method (Figure 7). For individual identification, we use the Awake data of 25 subjects who have data from two or more lecture sessions. We randomly select one facial image of each subject from the data of different lecture sessions and use them as Gallery (registered data) and Probe (test data), respectively. We compare the feature vector obtained by inputting a Probe into the estimation model with the feature vectors obtained by inputting each subject's Gallery into the model, and estimate that the subject whose feature vector is most similar to the Probe is the same person. However, the feature vector is V_{state} for the proposed method and V_{face} for the comparison method, and the similarity of the feature vectors is obtained using cosine similarity. Individual identification is performed for each Probe and the percentage of correct recognition is calculated. The trials were repeated 100 times and the averages of the recognition accuracy are shown in Table 8. Lower recognition accuracy values indicate better performance, and the proposed method's lower accuracy confirms the deviation module effectively separates individual features.

5 CONCLUSION

In facial expression recognition, individual facial feature differences and expression methods can negatively affect recognition accuracy. This study proposes a method using a deviation module to reduce the impact of individual differences, especially for estimating ambiguous internal states, which are more challenging than basic emotions. To handle subtle and ambiguous expression changes, we also utilize *mixup* for data augmentation. Evaluation on e-learning facial images for drowsiness estimation showed that using the deviation module improved accuracy, confirming its effectiveness in handling individual differences. Applying *mixup* further enhanced accuracy, with the best results achieved when mixing state feature vectors for the same individual.

REFERENCES

Cao, Q., Shen, L., Xie, W., Parkhi, O. M., and Zisserman, A. (2018). Vggface2: A dataset for recognising faces across pose and age. In *2018 13th IEEE International Conference on Automatic Face and Gesture Recognition (FG 2018)*, pages 67–74.

Friesen, W. V. (1973). Cultural differences in facial expressions in a social situation: An experimental test on the concept of display rules.

Kim, J.-H., Kim, B.-G., Roy, P. P., and Jeong, D.-M. (2019). Efficient facial expression recognition algorithm based on hierarchical deep neural network structure. *IEEE Access*, 7:41273–41285.

Liu, X., Vijaya Kumar, B., Jia, P., and You, J. (2019). Hard negative generation for identity-disentangled facial expression recognition. *Pattern Recogn.*, 88(C):1–12.

Meng, Z., Liu, P., Cai, J., Han, S., and Tong, Y. (2017). Identity-aware convolutional neural network for facial expression recognition. In *2017 12th IEEE International Conference on Automatic Face & Gesture Recognition (FG 2017)*, pages 558–565.

Schroff, F., Kalenichenko, D., and Philbin, J. (2015). Facenet: A unified embedding for face recognition and clustering. In *2015 IEEE Conference on Computer Vision and Pattern Recognition (CVPR)*, pages 815–823.

Szegedy, C., Ioffe, S., Vanhoucke, V., and Alemi, A. A. (2017). Inception-v4, inception-resnet and the impact of residual connections on learning. In *Proceedings of the Thirty-First AAAI Conference on Artificial Intelligence*, AAAI'17, page 4278–4284. AAAI Press.

Xie, S., Hu, H., and Chen, Y. (2021). Facial expression recognition with two-branch disentangled generative adversarial network. *IEEE Transactions on Circuits and Systems for Video Technology*, 31(6):2359–2371.

Zhang, H., Cisse, M., Dauphin, Y. N., and Lopez-Paz, D. (2018). mixup: Beyond empirical risk minimization. In *International Conference on Learning Representations*.

Zhang, H., Jolfaei, A., and Alazab, M. (2019). A face emotion recognition method using convolutional neural network and image edge computing. *IEEE Access*, 7:159081–159089.

Zhang, K., Zhang, Z., Li, Z., and Qiao, Y. (2016). Joint face detection and alignment using multitask cascaded convolutional networks. *IEEE Signal Processing Letters*, 23(10):1499–1503.

Zhang, W., Ji, X., Chen, K., Ding, Y., and Fan, C. (2021). Learning a facial expression embedding disentangled from identity. In *2021 IEEE/CVF Conference on Computer Vision and Pattern Recognition (CVPR)*, pages 6755–6764.